Assessment of the Indian Ocean bigeye tuna stock using CASAL

R.M. Hillary[1]
Dept. of Biology, RSM,
Imperial College London, SW7 2BP, UK.
I. Mosqueira,
AZTI Fundazioa,
Sukarrieta, Bizkaia, Spain.

July 2006

1 Assessment model

CASAL is an statistical catch-at-age (or catch-at-length) model that is able to integrate various sources of information in the estimation procedure (Bull *et al.*2005). The assessment population dynamics as applied in the present assessment are age-structured (with ages ranging from 0-18), and seasonal. This allows 0-group recruitment dynamics to be explicitely considered. The spawning season is reduced to an instantaneous event at the the beginning of the year, while recruitment and fishing occur in the following season, which encompasses the rest of the year. The CASAL package (Bull *et al.*2005) can estimate fishing mortality, but we have chosen to use the harvest rate option, which uses selectivity and catch biomass to calculate the harvest rate-at-age - this avoids the requirement of estimating annual F values. See the Appendix for the specifics of the exploitation dynamics.

Recruitment to the population is modelled using a Beverton-Holt stock-recruit function with a fixed steepness, initially assumed to be h=0.8. Conditions at the start of the time series are assumed to be at unexploited equilibrium. Two types of selectivity ogives were applied: double-normal (bell shaped) and free selectivity, where a single selectivity

[1]E-mail: r.hillary@imperial.ac.uk

parameter is estimated for each age class. This option was used for the purse seine and artisanal fleets, because standard selectivity curves could not fit the catch-at-age patterns observed in the data, with the highest proportions in the catch corresponding to the younger ages.

An alternative run was considered were the catches obtained by the artisanal fleets were introduced in the model, despite being a small percentage of the total catch (around 1% in 2004). Observation of the patterns in the catch-at-age estimates for these fleets (Fig. 1) shows the existence of three distinctive regimes in the temporal dynamics of this fleet aggregation: (a) the first, from 1950 to 1964; (b) the second, from 1965-1969; (c) and the latest, from 1970 to the present. For each of these periods, a separate "free" selectivity curve was estimated, to factor in these observed changes.

Inter-annual deviations from the stock-recruit curve are not estimated, and the reasons for this choice require further explanation and graphical assistance, and will be detailed later on.

Estimated parameters in this model implementation are virgin spawner biomass, B_0, and the three fleet's selectivity parameters. This gives a total of 10 parameters for the two-fleet base case scenario, and a maximum of 27 for the runs including the artisanal fleets.

The estimation method is Bayesian, thus requiring prior distributions for parameters to be specified. The values and reasons for the choice of priors are detailed further on in the document. Three tuning data sets are modelled in the likelihood function: the index of abundance, in this case the Japanese long-line standardized CPUE series (Okamoto, 2006); and the purse seine and longline (and artisanal where relevant) age frequency data. The index of abundace is assumed to be log-normally distributed, via a catchability parameter, around the model-predicted longline exploitable biomass. The observation CV assumed for these data was 15% - the same for all years, calculated from the CV in the log-residuals obtained when fitting a loess smoother through the data. This effectively detrends the CPUE data. The age frequency data was assumed multinomially distributed about the model-predicted age frequencies, with the yearly sample sizes pre-calculated

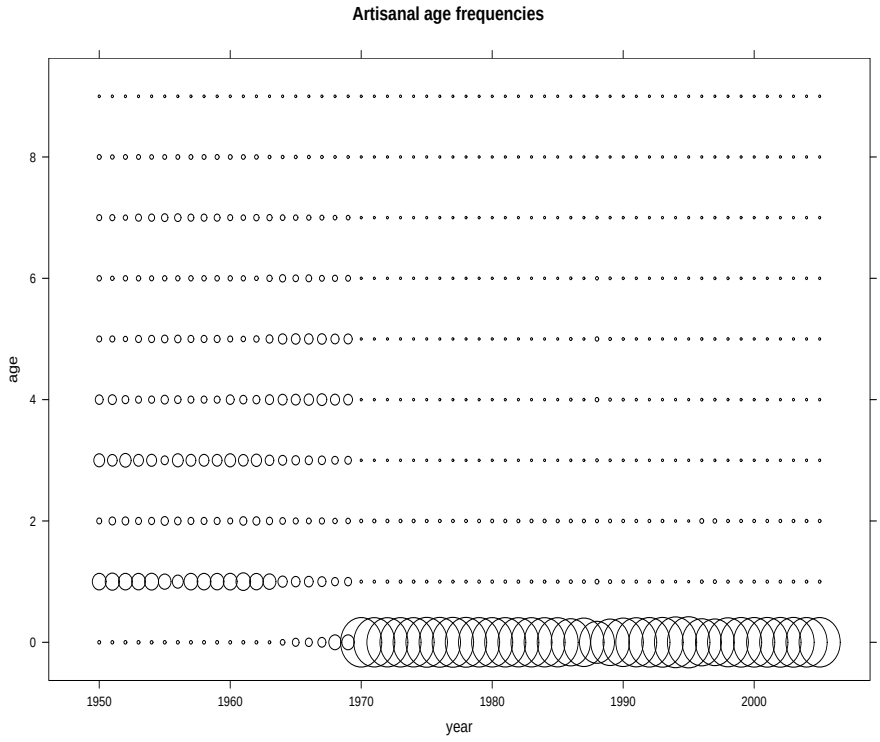

Figure 1: *Age frequencies for the artisanal fleet. There periods with different regimes can be considered here, from 1950-1964, 1965-1969 and 1970 to the present.*

and re-adjusted later, in line with commonly accepted statistical weighting procedures.

CASAL employs a variant of the ADOL-C automatic differentiation (AD) library, based upon the same methodology used by other modelling software such as AD Model Builder. Like all gradient-based minimisation routines, CASAL requires sensible initial guesses. Exploratory fits to the data were carried out. Visual inspection of the results was used to choose a set of initial values for the actual model runs. Convergence of the estimation routine was confirmed both by the CASAL software itself, and by inspection of various minimisation outputs, which can very quickly show non or false convergence. The overall minimisation takes only a few seconds with a sensible initial guess.

2 Exploratory data analysis and data weighting

For this assessment, we have four main data sources: catch-at-age data for the long-line, purse seine and artisanal fleets, and the long-line standardized index of abundace. As already outlined, we are working in a Bayesian framework, and with multiple data sources, we must be sure that we are sensibly weighting the data in the likelihood function. A common approach is to use multiplicative weights, for each of the data sets, usually in a least squares procedure. In the assessment model presented here, however, sensible weighting paratemerts are derived from initial analyses of the data.

Catch-at-age data, for both fleets, is treated as proportions-at-age data, and a multinomial distribution is assumed. Given the observed, $p_{y,a}$, and the model-predicted, $\widehat{p}_{y,a}$, catch-at-age proportions (for both fleets), the likelihood function is defined as

$$L_C = \prod_y \prod_a (\widehat{p}_{y,a})^{\widehat{N}_y p_{y,a}}, \tag{1}$$

where $\widehat{N}_y$ is the effective sample size for that year. The effective sample size reflects the "true" independent level of sampling which gave rise to the catch-at-age data, given that not all fish caught are sampled. We can calculate an initial estimate of $\widehat{N}_y$ from the

proportions data, using the following equation:

$$cv_a = \frac{\sqrt{\widehat{N}_y p_{y,a}(1 - p_{y,a})}}{\widehat{N}_y p_{y,a}} \tag{2}$$

where the CV-at-age, cv_a can be calculated using direct or bootstrap methods. Equation (2) can be solved (using Newton-Raphson methods) for $\widehat{N}_y$, thus providing an initial estimate of the effective sample size by year, for both fleets.

We now need to decide on the CV by year, for the CPUE data. For this, ideally we would have some estimate of this CV using either a bootstrap procedure, or directly from a GLM for example. If we do not have such an estimate, there are ways to obtain this estimate from the data themselves. If we simply computed the sample variance in the CPUE data, we will almost certainly over-estimate the variance, as we are implicitly assuming no trend in the data. What we did was to first de-trend the data (using a loess smoother) and then look at the CV in the log-residuals resulting from the smoothing process. This is then a reasonably sensible weighting factor for the CPUE data in the likelihood. The value we used, all years, was a CV of 0.15, based upon the approach described above.

2.1 Iterative re-weighting

The data weighting method we have just described is the first step in an iterative process. To ensure correct weighting of the input data, an assessment is performed using the initial weightings. The variance and sample size values are then inspected, as they are estimated from the observed and model-predicted observations. Fo the CPUE series, for example, a value for the CV of the residuals was assumed, but this can obviously be calculated from the residuals resulting from fitting the model to the data. If the estimation CV was much higher, then we should look at estimating a process error term (Hillary *et al.*, 2006), which characterises the extra level of uncertainty required by the model to fit to the data. As it turns out, our initial guess of around 15% CV was close (actual value was around

13%), so we can be reasonably sure we have weighted the CPUE correctly.

With regards to the catch-at-age data, we can compute the predicted sample size, $\widehat{N}_y$, from the following equation:

$$\widehat{N}_y = \frac{\sum_a \widehat{p}_{y,a}(1-\widehat{p}_{y,a})}{\sum_a (\widehat{p}_{y,a} - p_{y,a})^2}. \tag{3}$$

These updated values of $\widehat{N}_y$ can then be placed in the assessment model, which is run again, and then new values of $\widehat{N}_y$ are computed. Estimates of $\widehat{N}_y$ converge very quickly, and usually one updating step is enough.

2.2 Recruitment information

There is no fishery-independent survey data for this stock to provide year-class strength information, so all information on recruitment will potentially come from the commercial catch data. As mentioned before, inter-annual variations from the stock-recruit curve are not estimated, as the data available is not informative enough on the values of such parameters. Figures 2 & 3 show the catch proportions-by-cohort bubble plots, for the long-line and purse seine fleets, respectively.

As can clearly be seen from Figs. 2 & 3, there are no obvious consistently strong or weak year-classes moving down any of the cohorts. Given that the longline CPUE data is an aggregated index of catch and effort trends in the long-line fleet, and the catch-at-age data for this fleet display little if any recruitment information, then we cannot realistically expect the CPUE data (which is age-aggregated) to contain information on recruitment trends. If we allowed the model to estimate inter-annual variations in recruitment, the model could fit very closely to the CPUE data, even at the danger of overfitting to it.

There is a certain amount of observation error included in such indices as CPUE - in our analysis, we used an *ad hoc* de-trending method to obtain an observation error CV of 15%. This CV can be considered reasonable, if perhaps even a little optimistic. Allowing

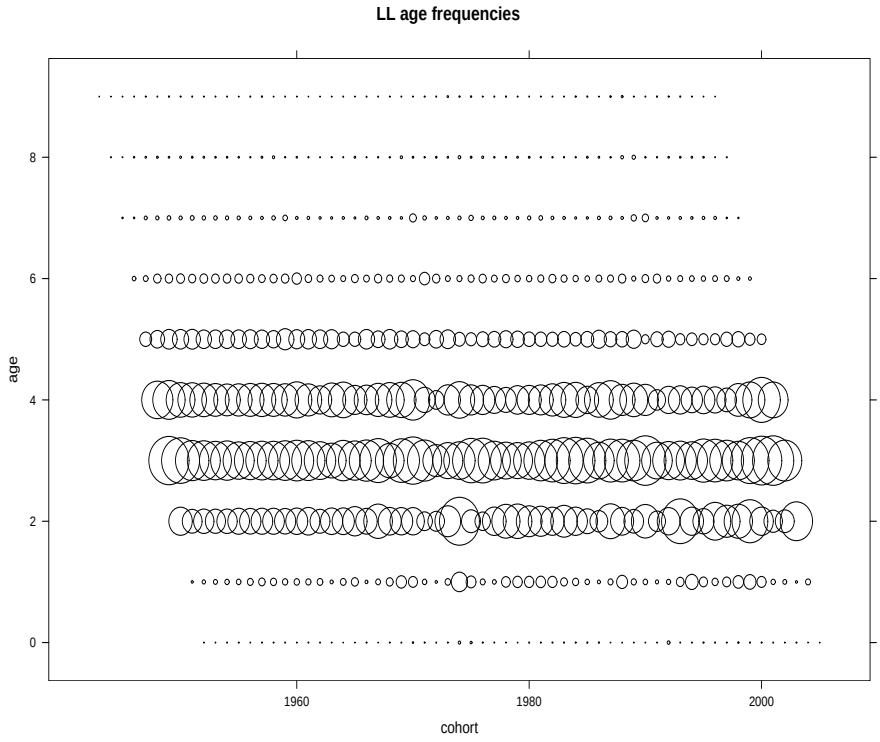

Figure 2: *Long-line catch-at-age proportions by cohort, for the most selected ages. As we can see, there are no obvious consistently strong or weak cohorts moving through the data.*

recruitment to vary, a CV of 5% could easily be obtained, a value that is likely to indicate an overfitting problem. This very issue of estimating sensible and reliable recruitment trends, given data that do not seem to possess any information on such processes, was looked at thoroughly by Hillary *et al.*(2006). It was concluded that it was more sensible not to estimate these recruitment variations, and to use stochastic recruitment variations when projecting the stock forward, under certain catch scenarios, and to begin these randomisations at the beginning of the assessment period. This is a crude, but simple attempt to include uncertainty in the stock dynamics - both historically and in the future.

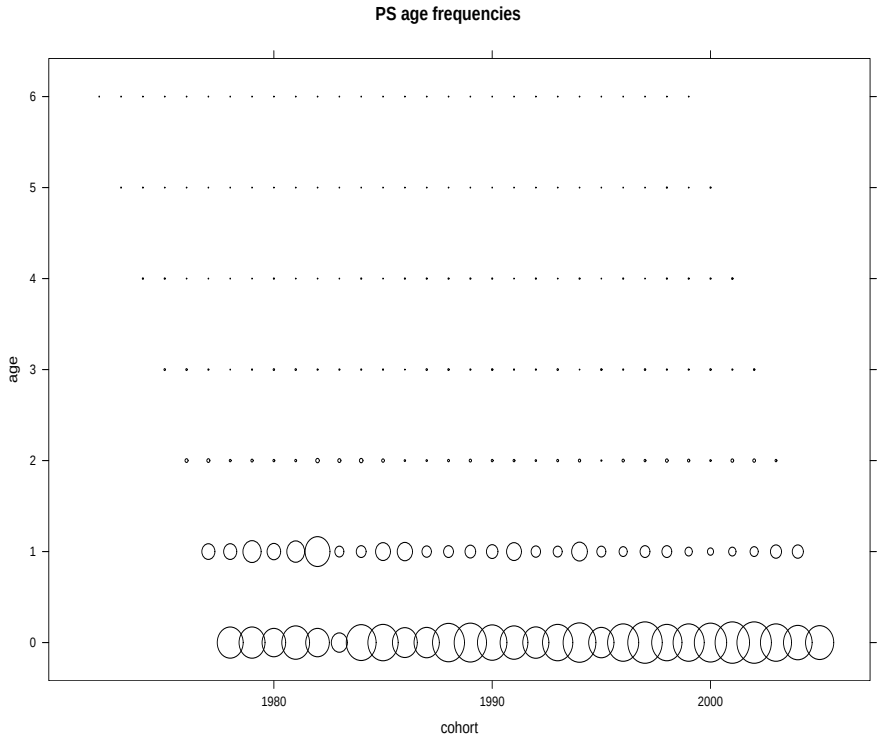

Figure 3: *Purse seine catch-at-age proportions by cohort, for the most selected ages. As with the long-line fleet, there are no obvious consistently strong or weak cohorts moving through the data.*

2.3 Priors

We must assign prior distributions to each of our parameters in a Bayesian analysis. For the CPUE catchability coefficient, we assumed a log-uniform prior, which is a standard non-informative prior for such a scale parameter and a log-normal likelihood (Box & Tiao, 1973). For the virgin spawner biomass, B_0, a log-uniform prior, with lower and upper bounds set at 1000 and $5{\times}10^6$ tonnes, respectively, was assumed. Uniform priors were applied to all the selectivity parameters. For the the double normal parameters, $(a_{\max}, s_L, s_R)$, used for the long-line fleet lower and upper bounds of $(0.05, 0.05, 0.05)$ and $(50, 50, 500)$ were set, respectively. For the free selectivity parameters, estimated for the

purse seine and artisanal fleets, lower and upper bounds of zero and one, respectively, were defined.

3 Results

For our base-case assessment run, natural mortality, growth parameters and maturation values used in previous assessments were applied, with the steepness value of the stock-recruitment relationship fixed at $h = 0.8$. Four sensitivity scenarios have also been considered: changes in the assumed value of the steepness parameter, changes to the vector of natural mortality-at-age, analysis of any retrospective trends in the base-case assessment, and the inclusion of the catches obtained by the artisanal fleets.

3.1 Base-case summary

In Fig. 4, the fit obtained to the CPUE, along with other standard regression information is presented. A reasonably good fit to the long-line CPUE is achieved - it should be noted that the CV in the residuals is 13%, which is slightly less than that assumed in the estimation method. This indicates that the population model is not under-fitting to these data, and that no more freedom is required in the dynamics to explain the data - if the assumption of an observation error of 15% is considered appropiate. If available, yearly estimates of the error in each of the CPUE points, obtained using GLM or GLMM approaches, can be incorporated.

Fits to the long-line and purse seine age frequencies can be found in Figs. 5 & 6, respectively. The fits appear to be good to both data sets, with only few years where the model cannot fully capture the observed age distribution of the catches from both fleets. The estimated selectivity curves can be found in Fig. 7, and are very similar to those used in the previous assessment. We do not show the fits to each of the artisanal fleets, but they are also very good, with little or no observable bias.

An overview of the stock dynamics and current stock status can be found in Fig. 8. SSB

appears to be currently just below 50% of virgin levels, but above 20% - the SSB depletion, B_{2005}/B_0, is estimated to be 43%. The long-line exploitable biomass is currently at just above 50% virgin levels. Expected recent recruitment levels are at around 90% of those seen at unexploited equilibrium, with current harvest rates settling just below 0.2 - this equates to a total level of F_y of just above 0.2.

3.2 Sensitivity trials

With regards to sensitivity of the assessment model to the assumed value of the steepness, two alternative values of 0.7 and 0.9 were used. For a lower/higher value of steepness, one sees a corresponding higher/lower value in the estimated value of B_0 - this is because B_0 and h are negatively correlated (Table 1).

As for alternative natural mortality-at-age vectors, we used two alternatives: the first had an increase in the zero group, with $M_0 = 1.2$; the second looked at lower juvenile natural mortality, with $M_{0,1} = 0.6$. With a change in M, two changes almost always occur, and this case is no different. When the level of M increases, we see a decrease in B_0; the second change is in the estimated selectivity patterns (only above the ages at which M has been altered), to account for the change in the cohort structure caused by the higher value of M - vice versa for a decrease in M.

The reason for the observed changes in B_0 are detailed in Hillary *et al.*(2006), and relate to the definition of R_0 in the population model. We have that $R_0 = \rho^{-1}B_0$, where ρ is the SSB per unit recruit. Given an increase in natural mortality, we can obtain quite a strong decrease in the value of ρ, and to obtain a roughly similar R_0 as the base-case (this is required to fit to the data) we see an decrease in B_0 to compensate for the change in ρ. The exact opposite occurs for a decrease in M. Table 1 summarises the key parameters and quantities for the base-case and sensitivity tests.

Retrospective analyses provide information on how new data is informing the assessment parameters, and we performed a standard 3 year (back to 2002) retrospective analysis, as this was the last year this particular stock was assessed. Figure 9 shows the resulting

Table 1: Sensitivity summary table.

Model	B_0	R_0	B_{2005}/B_0
Base-case	1.86×10^6	9.59×10^7	0.43
$h = 0.7$	1.94×10^6	1.01×10^8	0.42
$h = 0.9$	1.79×10^6	9.26×10^7	0.43
$M_0 = 1.2$	1.82×10^6	1.41×10^8	0.44
$M_{0,1} = 0.6$	2.05×10^6	7.11×10^7	0.43

SSB trajectories.

As we can see from Fig. 9, there is a clear, consistent upward revision in the estimated SSB trajectory from 2002 to 2004, but hardly any change from 2004 to 2005. Also, there is very little change in the SSB depletion factors, B_{current}/B_0, with all of them lying between 0.42 and 0.44. There are also some small changes in the estimates of selectivity for each of the fleets, but not of any real significance. This suggests that these data are providing a reasonably consistent assessment, with only minor changes in absolute abundance, and very little change in estimated stock depletion levels.

With regard to the incorporation of the artisanal fleet catches, the age frequency data is well fitted (given the previously defined temporal split of these data), but the only significant difference we see in the results is a slight increase in the estimated value of B_0 (an increase from 1.86 to 1.92 million tonnes), with no perceptible changes in estimated selectivity patterns or depletion levels.

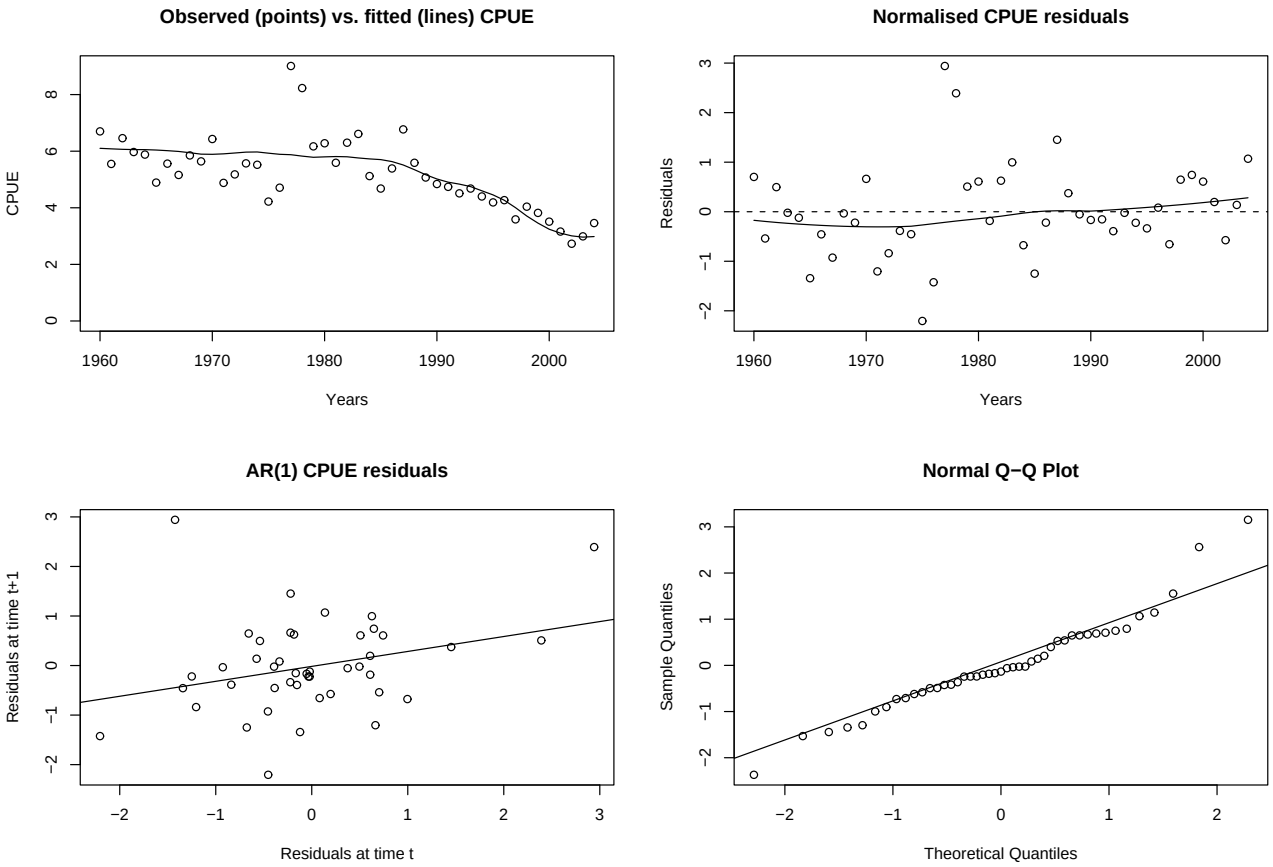

Figure 4: *Observed vs. predicted CPUE (top left); residuals and their temporal trend (top right); residual autocorrelation trend (bottom left); and residual QQ plot (bottom right).*

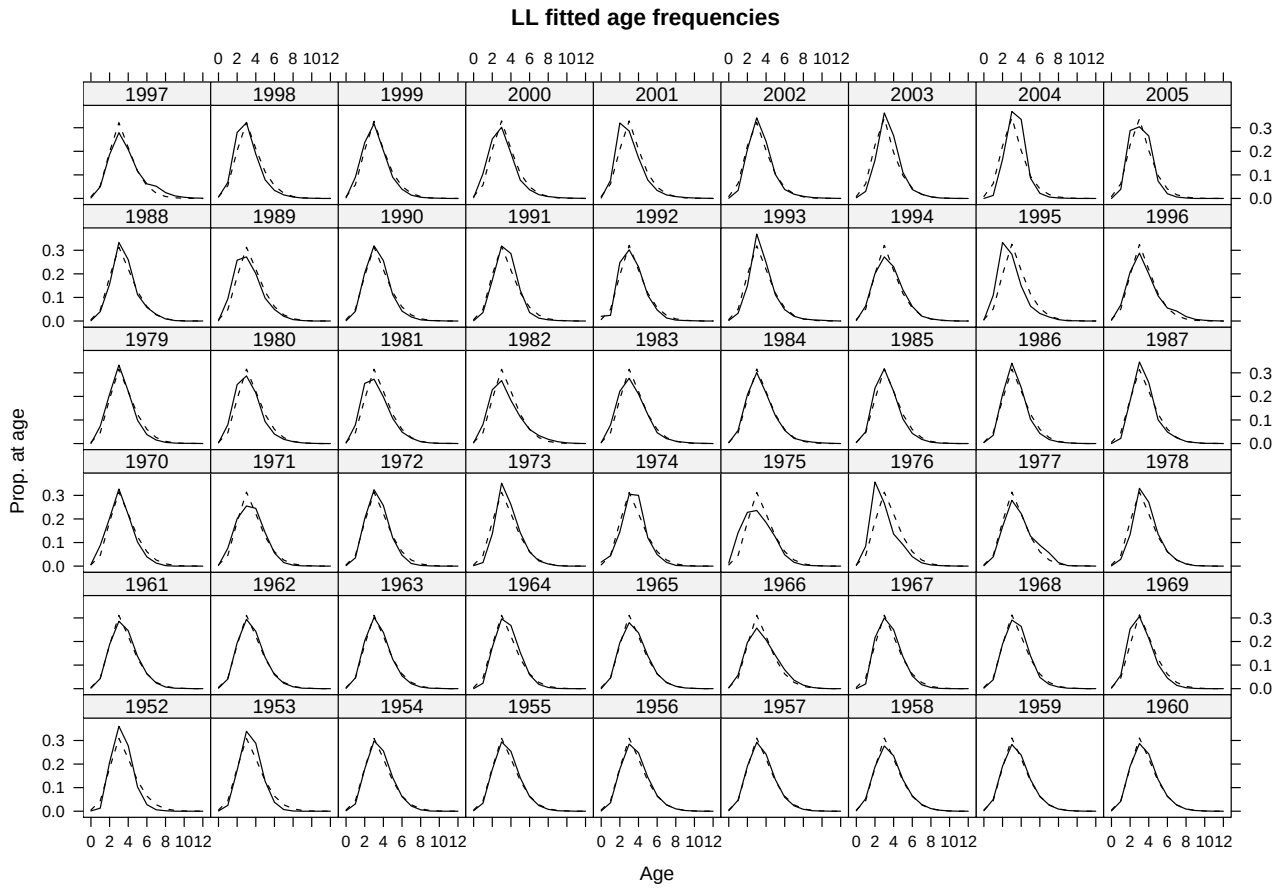

Figure 5: *Fits to the long-line age frequency data - observed and predicted frequencies are given by the full and dashed lines, respectively.*

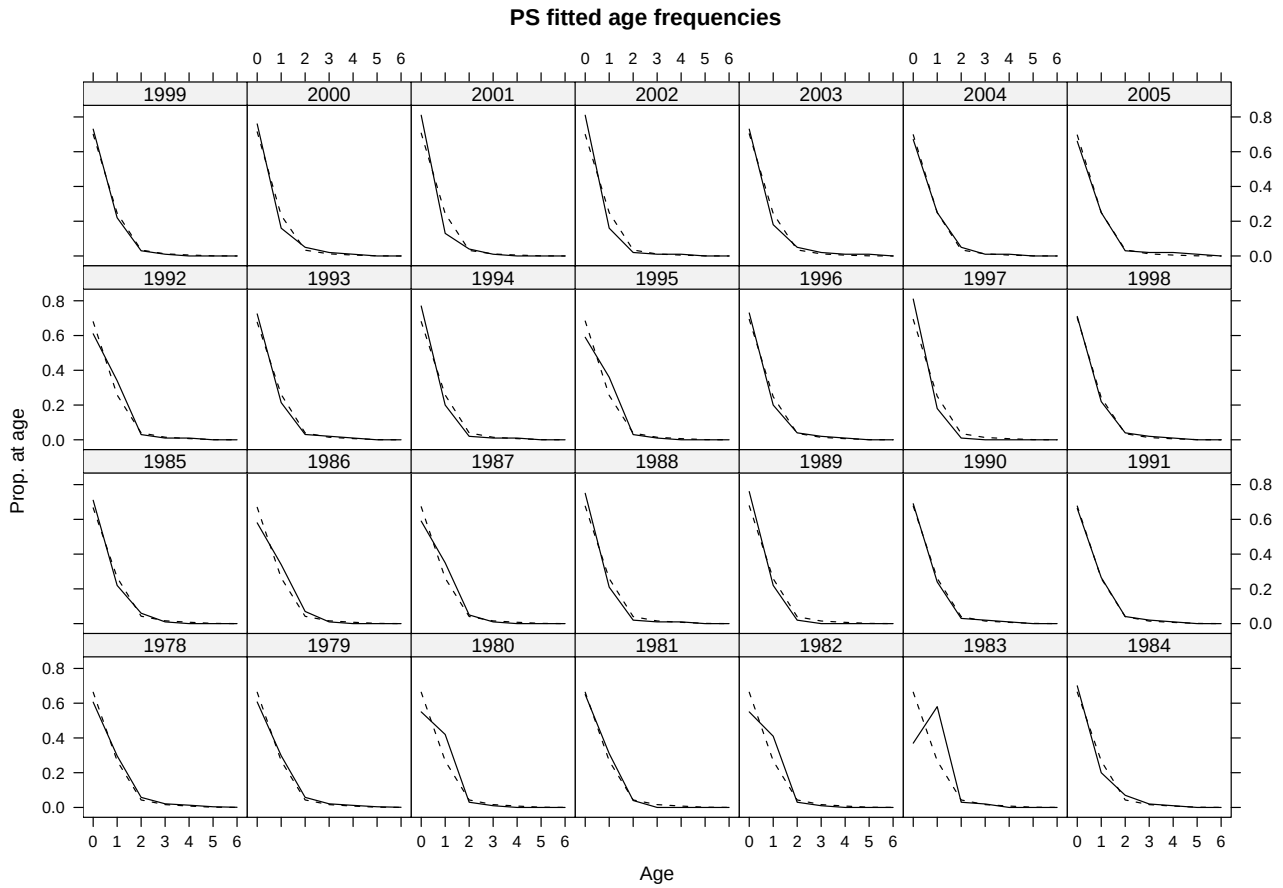

Figure 6: *Fits to the purse seine age frequency data - observed and predicted frequencies are given by the full and dashed lines, respectively.*

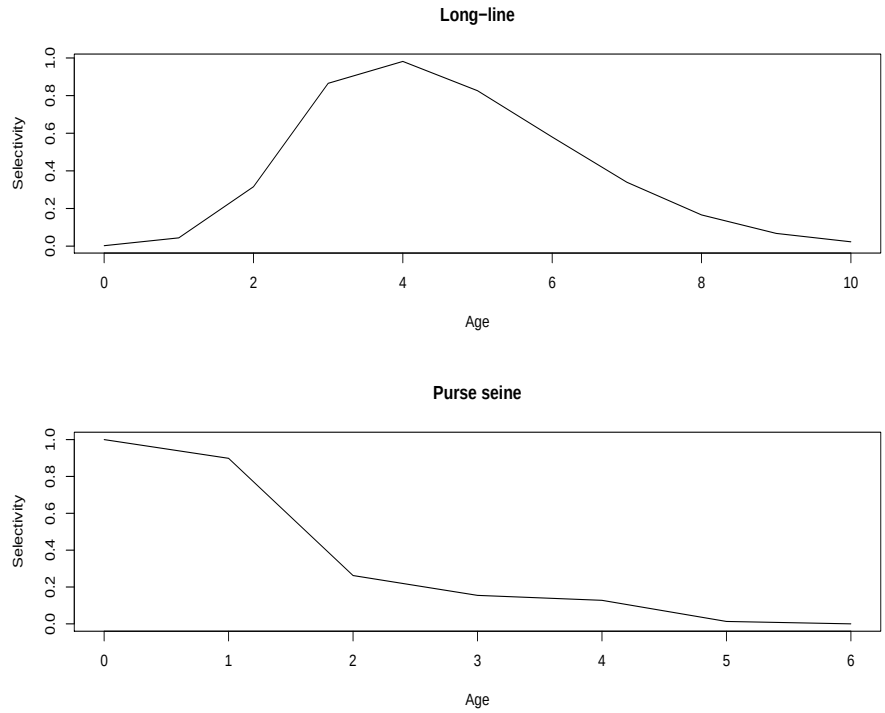

Figure 7: *Estimated long-line (upper) and purse seine (lower) selectivities.*

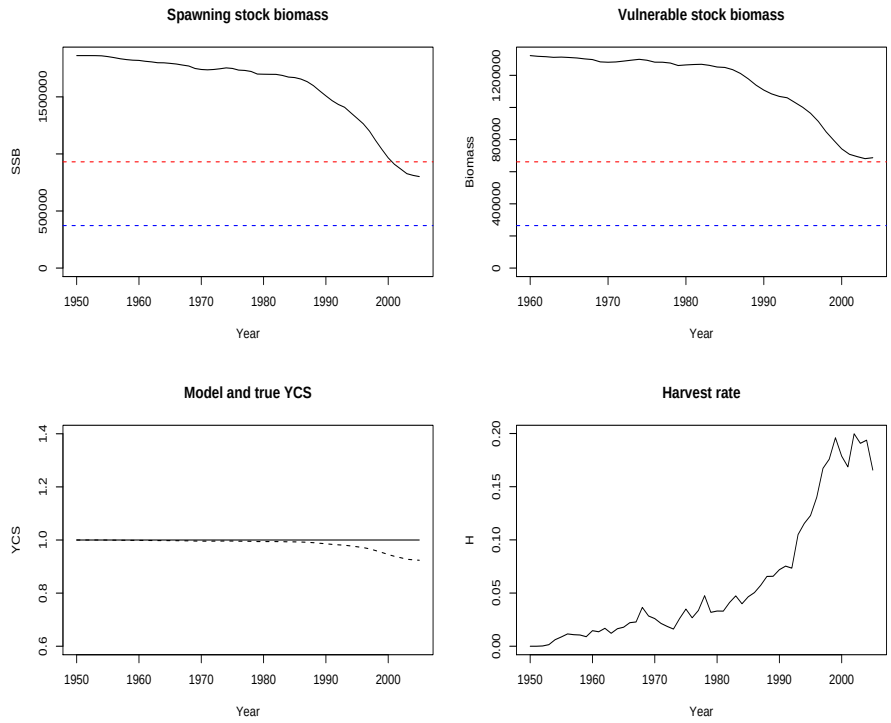

Figure 8: *SSB dynamics (top left), long-line exploitable biomass (top right), recruitment reduction from virgin (bottom left), and the overall harvest rate (bottom right). The red and blue lines represent 50% and 20% of virgin conditions, respectively. The harvest rate shown here is for the long-line fleet.*

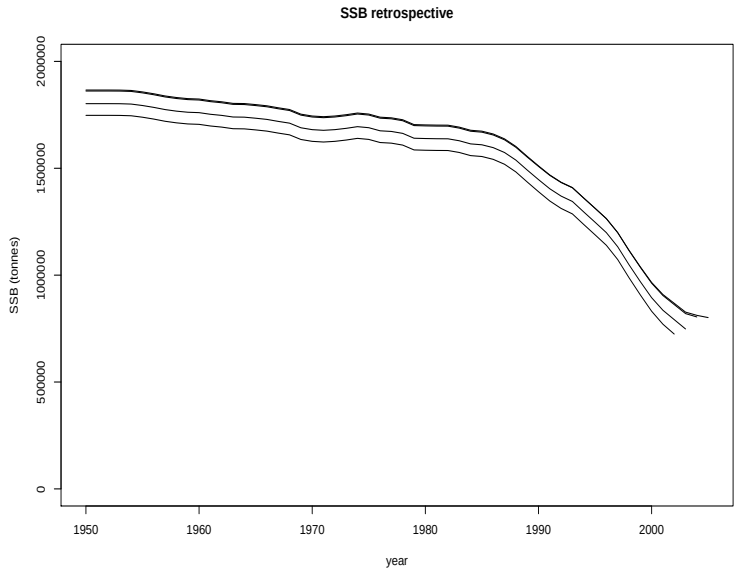

Figure 9: *Three year retrospective SSB trajectories. We see consistent revisions upwards of the SSB levels from 2002 to 2004, but vey little change between 2004 and 2005.*

4 Stock status & projections

CASAL allows computation of MSY information and projections for various catch levels. For the base-case scenario, a catch-split for each of the current fisheries, based on the latest relative levels of catch, wss assumed. A catch ratio of 0.76 and 0.24, for the long-line and purse seine fleets, respectively, was used. Assuming deterministic conditions, we found that $C_{MSY} = 0.07113 \times B_0 = 132,404$ tonnes, $B_{MSY} = 0.247 \times B_0 = 459,406$ tonnes, with $H_{MSY} = 0.288$.

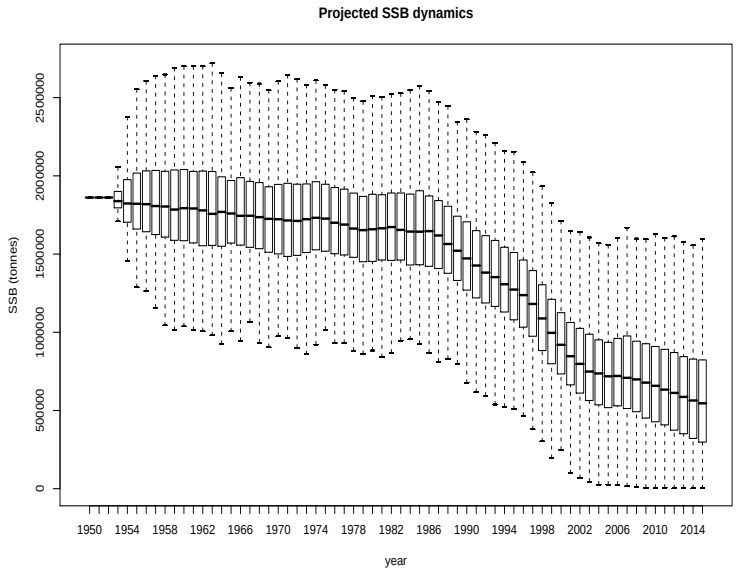

Figure 10: *Historic and future simulated SSB, assuimg constant future catches of 105,000 and 29,000 tonnes for the long-line and purse seine fleets, respectively. The centre line is the median, with the first box defining the first inter-quartile range, and the whiskers defining the 95% confidence intervals.*

Projections have also been carried out. First, a simple 10 year projection, based on catches fixed at 2002 levels - 105,000 tonnes for long-line, 29,000 tonnes for purse seine - was performed to assess how current catch levels would affect the future population size and structure. Status quo catches were taken as those observed in n2002, given the

temporal changes to the fishery observed 2003 and 2004, related to the high abundance of yellowfin tuna. As mentioned before, to account for some stochasticity in the historical and future dynamics, we randomised the recruitment dynamics, using log-normal, non-autocorrelated variates, assuming a CV of 0.5. Figure 10 shows the simulated SSB dynamics, assuming a constant catch for each fleet, projecting forward for 10 years.

As observed in Fig. 10, current catch levels (for each fleet) cause further depletion of the levels of SSB, with the probability of future SSB being less than B_{MSY} rising from 0.19 in 2006, to 0.399 in 2015.

References

Box, G. E. P amd Tiao, G. C. (1973) Bayesian inference in statistical analysis. Wiley, New York.

Bull, B., Francis, R.I.C.C., Dunn, A., McKenzie, A., Gilbert, D. J. and Smith, M. H. (2005) CASAL User Manual v2.07-2005/07/06. NIWA Technical Report **126**.

Hillary, R. M., Kirkwood, G. P., Agnew, D. J. (2006) An assessment of toothfish in Subarea 48.3 using CASAL. *CCAMLR Science* (in press).

Appendix: exploitation dynamics

In the CASAL assessment model, we use harvest rates, and not fishing mortality, to define the exploitation dynamics, for the given fleets. Since this is different from the approach used in the ASPM model, previously used to assess this stock, we will give a simple overview of how the harvest rates are calculated in the assessment.

Given a total catch (in weight) for each fleet, $C_{f,y}$, and a selectivity function, $s_{f,a}$, we define biomass open to exploitation by this fleet as follows:

$$EB_{f,y} = \sum_a N_{y,a} e^{-M_a/2} s_{f,a} w_a, \tag{4}$$

where w_a is the weight-at-age of the animal, M_a is the natural mortality-at-age, and $N_{y,a}$ are the model-predicted numbers-at-age. We can now define the total harvest rate:

$$H_{f,y} = \frac{C_{f,y}}{EB_{f,y}}, \tag{5}$$

leading to the harvest rate-at-age (by fleet):

$$h_{f,y,a} = H_{f,y} \times s_{f,a} \tag{6}$$

In the simplest one-season model, the exploitation dynamics proceed as follows:

$$N_{y+1,a+1} = N_{y,a} e^{-M_a} \left(1 - \sum_f h_{f,y,a}\right), \tag{7}$$

with the obvious extension when we are in the plus group age class.

Further sensitivity trials for the CASAL Indian Ocean bigeye tuna assessment

R.M. Hillary[1]
Dept. of Biology, RSM,
Imperial College London, SW7 2BP, UK.
I. Mosqueira,
AZTI Fundazioa,
Sukarrieta, Bizkaia, Spain.

July 2006

Details

During the presentations of the various assessment models, some issues were raised, with respect to the assumed natural mortality vector, and we now have the availability of the recalculated Taiwanese long-line fleet. With respect to the natural mortality vector, two alternative options were considered - both implement a type of inverse-bell shape (known as a cosh-type curve), to account for a decrease in M from juveniles to fully recruited fish, with an increase in M at the older ages, with the second suggested vector employing a senesence effect. These natural mortality vectors can be found in Table 1.

Table 1: Table of suggested natural mortality vectors for Indian Ocean bigeye tuna.

Age	0	1	2	3	4	5	6+
No senesence	1	0.6	0.3	0.4	0.4	0.4	0.4
Senesence	1	0.6	0.3	0.4	0.4	0.4	0.6

Figure 1 shows the mean-standardised long-line CPUE indices for all Indian Ocean

[1]E-mail: r.hillary@imperial.ac.uk

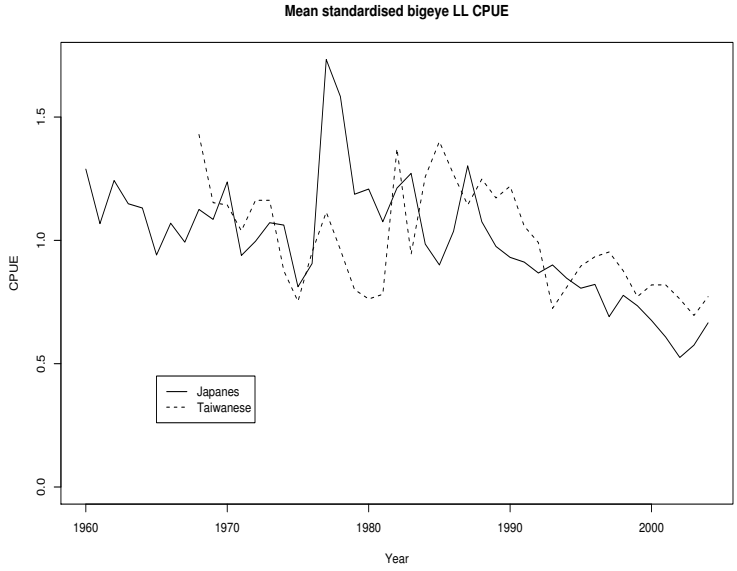

Figure 1: *Mean standardised long-line CPUE indices, for all Indian Ocean bigeye tuna, for the Japanese and Taiwanese fleets.*

bigeye tuna, for the Japanese and Taiwanese fleets.

To assess the sensitivity of the base-case assessment to the alternative natural mortality, we simpy re-ran the asessment model using these two vectors. With respect to the two alternative long-line CPUE series, we look at using the Taiwanese series on its own, and also the effect of using both series together. Table 2 presents a summary of these sensitivities, concentrating on relevant current-to-virgin and current-to-MSY information.

With respect to the alternative natural mortality vectors, the observed changes in B_0 occur due to the reasons outlined in our original document. Overall SSB depletion levels (B_{2005}/B_0) are the same as those in the base case assessment. One interesting observation is how the changes in natural mortality affect the estimates of C_{MSY}:

For the no senesence case, although we have a slightly higher M on age zero fish, it is lower on ages 1 and 2 than for the base case. This alters the yield-per-recruit behaviour, allowing for higher values of yield at MSY. When we add the senesence term, we effectively

Table 2: Summary table for the M and CPUE sensitivity trials. All biomass levels are given in tonnes. Cases TW and TW+JAP correspdond to using the Taiwanese CPUE and the Taiwanese and Japanese LL CPUE series, respectively.

Case	B_0	B_{2005}/B_0	C_{MSY}	H_{MSY}	B_{2005}/B_{MSY}	H_{2005}/H_{MSY}
Base case	1.86×10^6	0.43	132,404	0.29	1.74	0.58
No senesence	2.07×10^6	0.43	162,006	0.31	1.72	0.49
Senesence	1.75×10^6	0.44	137,427	0.31	1.74	0.48
TW	2.34×10^6	0.56	170,322	0.31	2.35	0.35
TW+JAP	2.15×10^6	0.52	156,865	0.31	2.18	0.41

counteract this effect, because of the higher values of M on the older ages that are still selected by the long-line fleet (ages 6 to 10). Note that the two alternative M vectors yield very similar values of H_{MSY} and current-to-MSY ratios.

When using the Taiwanese long-line CPUE data alone, we see a clear increase in the expected stock levels - both B_0 and B_{2005}/B_0 are larger than for the base case; as a result, and given we have not changed M or any other parameters, the estimated value of MSY is larger than the base case, and the current SSB is predicted to be over twice the size of B_{MSY} with current harvest rate predicted to be just over a third of H_{MSY}. When including both the Japanese and Taiwanese CPUE data, unsurprisngly we see that the estimated stock abundance lies between those estimated when using these two series separately.

Conclusions

In conclusion, the inclusion of the alternative natural mortality vectors has little effect, with respect to stock depletion and current-to-MSY ratios. One thing to note though is that the senesence M vector yields a higher estimated value of C_{MSY}, because of changes

in the yield-per-recruit relationship, caused by an iteraction of M and selectivity. When including the Taiwanese CPUE data - either on its own or together with the Japanese data - we see a more marked difference in the estimated stock status and indicators:

Using the Taiwanese data alone, we get an increase in the virgin SSB, and a lower value of the estimated SSB depletion. This gives rise to increases in the estimated values of C_{MSY} and B_{MSY}, but a very similar value of H_{MSY}. The current-to-MSY ratio indicators all suggest that the stock is above B_{MSY}, and beneath H_{MSY}, but more so than is predicted in the base case assessment. When including both CPUE series, the estimated stock status is between that seen when using the individual CPUE series in the assessment - which is not very surprising, given they recieve similar weighting in the the likelihood, and display a similar depletion trend.

Projection scenarios for the CASAL Indian Ocean bigeye tuna assessment

R.M. Hillary[1]
Dept. of Biology, RSM,
Imperial College London, SW7 2BP, UK.
I. Mosqueira,
AZTI Fundazioa,
Sukarrieta, Bizkaia, Spain.

July 2006

Constant harvest rate scenarios

The base-case assessment model, for the bigeye CASAL assessment, was chosen to be that using the $M1$ natural mortality vector, seen in Table , and using the Japanese long-line CPUE series, and the long-line and purse seine catch-at-age data. Constant harvest rate scenarios were considered, based upon the following agreed cases:

1. Projection using the harvest rate estimated in 2004.
2. Projection using the harvest rate estimated in 2002.
3. Projection using the mean harvest rate, over the period 1998-2001.

Table 1: Suggested new natural mortality vector for Indian Ocean bigeye tuna.

Age	0	1	2	3	4	5	6+
$M1$	1	0.6	0.3	0.4	0.4	0.4	0.4

[1]E-mail: r.hillary@imperial.ac.uk

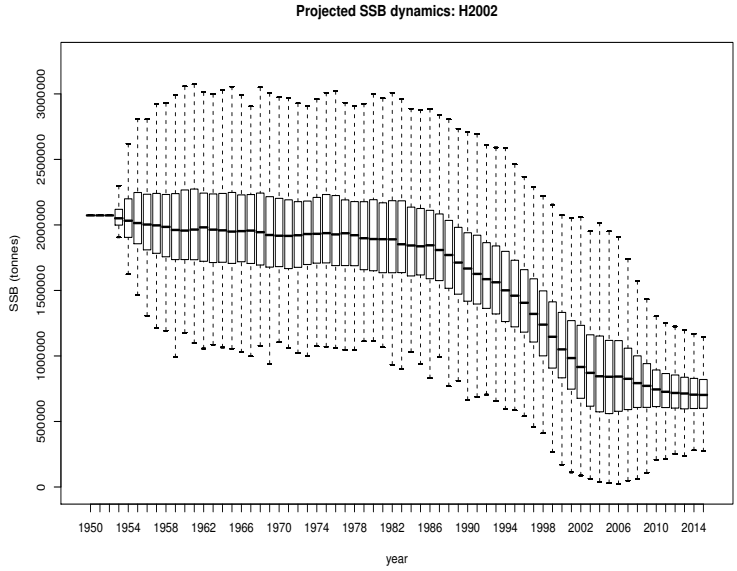

Figure 1: *SSB dynamics for case 1.*

We also looked at a projection using the maximum estimated harvest rate, from this particular CASAL model, which we refere to case case 4. For all projections, stochasticity was introduced into the dynamics (both historically and in the future), using log-normal non-autocorrelated deviates, with $\sigma_r = 0.5$. Figures 1, 2, 3 and 4 show the SSB dynamics for cases 1,2,3 & 4, respectively.

Constant catch scenarios

With respect to constant catch scenarios, we defined two cases:

1. Projection using 2004 long-line and purse seine catches.
2. Projection using a 10% reduction in the 2004 ling-line and purse seine catches.

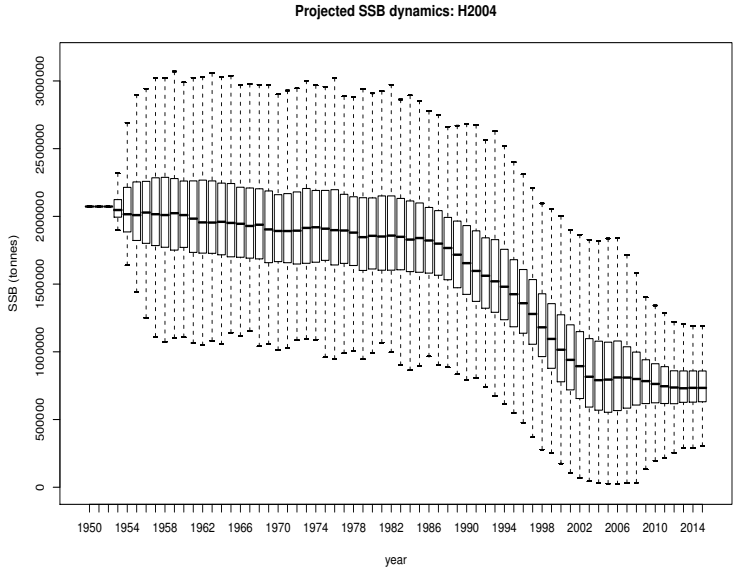

Figure 2: *SSB dynamics for case 2.*

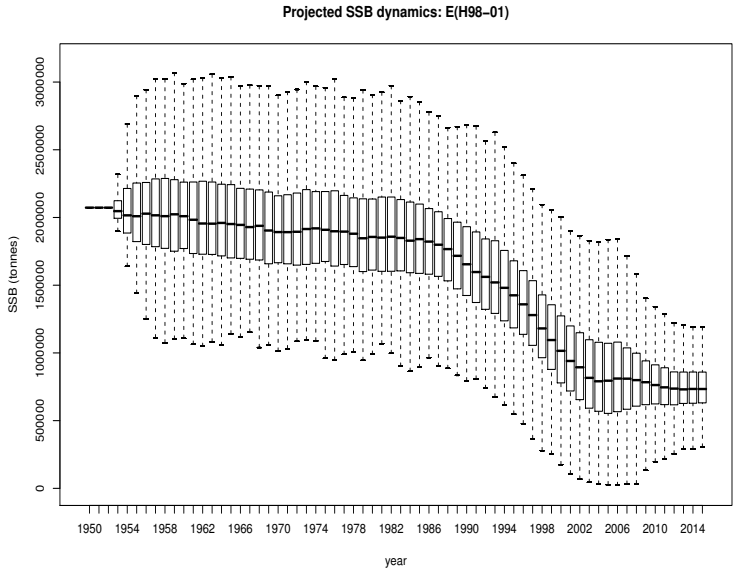

Figure 3: *SSB dynamics for case 3.*

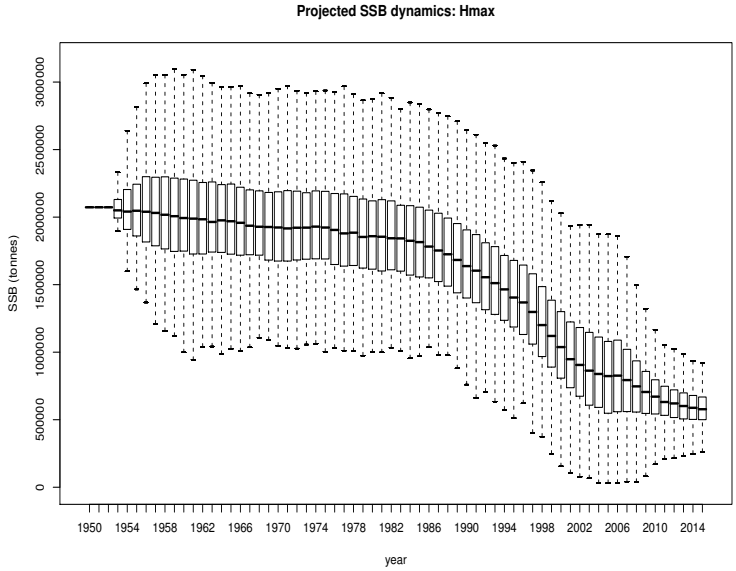

Figure 4: *SSB dynamics for case 4.*

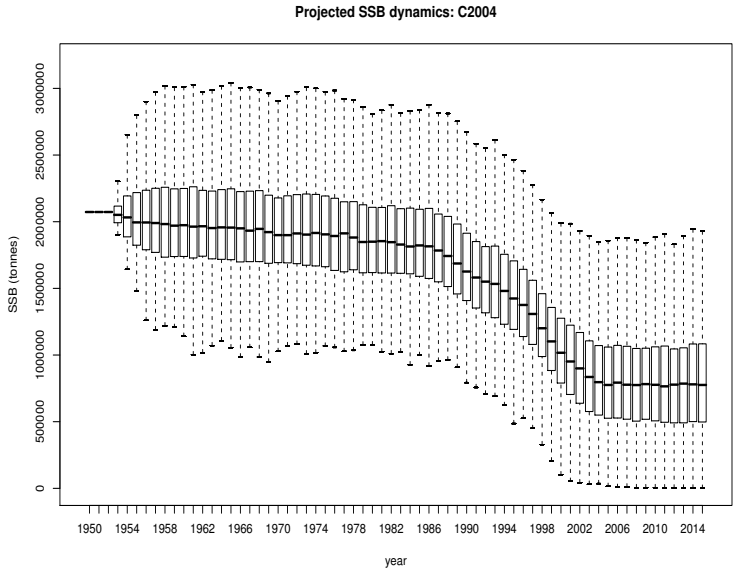

Figure 5: *SSB dynamics for constant catch case 1.*

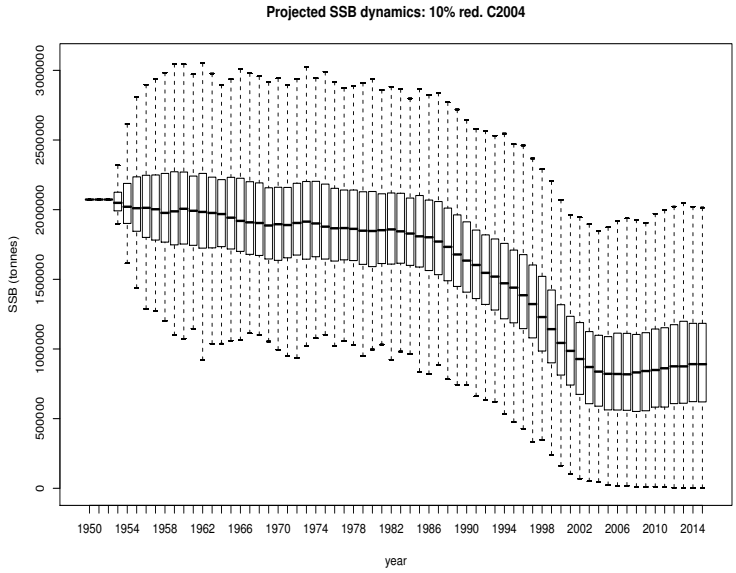

Figure 6: *SSB dynamics for constant catch case 2.*